Accepted for publication in ApJL

FU Orionis resolved by infrared long baseline interferometry at a 2-AU scale

F. Malbet, & J.-P. Berger
Laboratoire d'Astrophysique, Observatoire de Grenoble, UMR UJF/CNRS 5571

M.M. Colavita, M. Shao, J.K. Wallace, A.F. Boden, G.T. Van Belle, & D.W. Mobley
Jet Propulsion Laboratory, California Institute for Technology

C. Beichman
Infrared Processing and Analysis Center, California Institute for Technology and Jet Propulsion Laboratory

C.D. Koresko, S.R. Kulkarni, B.F. Lane, X.P. Pan
Palomar Observatory, California Institute for Technology

ABSTRACT

We present the first infrared interferometric observations of a young stellar object with a spatial projected resolution better than 2 AU. The observations were obtained with the *Palomar Testbed Interferometer*. FU Ori exhibits a visibility of $V^2 = 0.72 \pm 0.07$ for a 103 ± 5 m projected baseline at $\lambda = 2.2\mu$m. The data are consistent on the spatial scale probed by PTI both with a binary system scenario (maximum magnitude difference of 2.7 ± 0.5 mag and smallest separation of 0.35 ± 0.05 AU) and a standard luminous accretion disk model ($\dot{M} \sim 6 \times 10^{-5}$ $M_\odot$ yr^{-1}) where the thermal emission dominates the stellar scattering, and inconsistent with a single stellar photosphere.

Subject headings: stars: pre-main sequence — circumstellar matter — stars: individual (FU Ori) — accretion disks — instrumentation: interferometers — infrared: stars

1. Introduction

FU Orionis is the prototype of a class of young stellar objects (YSOs,) called *FUors,* that have undergone photometric outbursts of the order of 4-6 magnitudes in less than one year (Herbig 1966). A FUor's luminosity typically peaks at ~ 500 $L_{\odot}$, and then appears to decay on a 100-year timescale. FUors exhibit large infrared excesses, double-peaked line profiles, apparent spectral types that vary with wavelength, broad, blueshifted Balmer line absorption, and are often associated with strong mass-outflows (see Hartmann & Kenyon 1996 for a recent review on this phenomenon).

The FUors have been convincingly modeled as low-mass pre-main sequence stars (T Tauri stars) which are surrounded by luminous accretion disks. The inferred peak accretion rates are on the order of 10^{-4} $M_{\odot}$ yr^{-1}. The energy released by the accretion process is radiated at the disk surface, overwhelming the stellar emission. Kenyon & Hartmann (1991) showed that an opaque, dusty $A_v \sim 50$ mag infalling envelope with a cavity along our line of sight is consistent with both the mid-IR excess of FUors and the relatively low $A_v \sim 1 - 4$ mag estimated extinction of the inner source.

The radiative balance between disk emission and gravitational energy released by the accretion process implies that the disk's temperature falls with the $-3/4$ power of radius, leading to anticipated angular sizes on the order of one milliarcsecond in the near-IR at a distance of 450 pc. Malbet & Bertout (1995, hereafter MB95) therefore proposed using infrared long-baseline interferometry to probe the physics of these disks.

We present in this paper the first infrared interferometric observations of a YSO, taken with 4 milliarcsecond resolution at 2.2 μm using the *Palomar Testbed Interferometer (PTI).* The corresponding linear resolution is better than 2 AU at the 450 pc distance to FU Orionis. The object is found to be clearly resolved, with a fringe visibility significantly below unity and consistent with, although not unique to, the predictions of the disk model. Section 2 presents the observations and Section 3 the data processing. In Section 4, we discuss the results in the context of a number of models.

2. Observations

FU Orionis was observed from 1997 November 1 to 7 (nights 305, 306, 307, 309, 310, and 311) using the PTI. The PTI, located adjacent to the 200-inch Hale telescope on Palomar Mountain (California, USA), is a two-element interferometer with a 110-m baseline oriented roughly North-South. The observations were taken in the "single-star" mode, in which the measurement consists of the squared fringe visibility V^2 along the single baseline (Colavita et al. 1994). The fringe was tracked and measured in the K band for 11 scans of 125-130 sec each. Earth rotation provided a limited range of projected baselines: 98 m $\leq B \leq$ 108 m and $55° \leq \theta \leq 73°$. We used HD 42807 located at 9.4° from FU Ori as local calibrator star[1]. Scans of FU Ori were alternated with measurements of HD 42807 to ensure an accurate determination of the system visibility. We also used the other calibrator stars from the night to estimate the system visibility (see Sect. 3).

The apparent magnitudes for FU Orionis are V = 8.9, R = 7.7 and K = 4.6 mag. The object is close to the flux limit of both the acquisition and angle-tracking system and the fringe tracker, so special care was taken during the observations and data reduction to optimize sensitivity and avoid biasing the results. The instrument observing parameters were optimized for FU Ori, and identical settings were used for HD 42807. At the level of accuracy of this experiment, the global calibration is consistent with that obtained with the local calibrators.

3. Data processing

Because the faintness of FU Orionis made it necessary to operate in previously little-explored regimes close to the sensitivity limits of the instrument, we present the data reduction procedures and reliability tests here in some detail. The data processing essentially followed the steps detailed in Colavita (1998). We base our results on the spectrometer data rather than the white light data, since the high visibilities produced by its single-mode fiber and narrow bandpass outweighed the larger photon rate in the broadband "white-light" channel. To avoid introducing biases and to maximize sensitivity, we employed an incoherent estimator averaged over the entire K band. Examination of the other data products was used to help confirm the robustness of the final visibility measurement.

3.1. Calibrated visibilities

We obtained the *raw* square visibilities $V^2_{\rm raw} \sim 0.6 \pm 0.05$ for FU Ori. The critical next step in the processing consists of dividing the raw visibilities by an estimation of the instrument + atmosphere visibility (*i.e.,* the system visibility) to obtain *calibrated*

---

[1]Characteristics from Hipparcos catalogue (Perryman et al. 1997): V = 6.5, G8V, 55 mas parallax. Estimated K magnitude: 4.7; estimated diameter: 0.45 ± 0.03 mas.

visibilities V^2.

The single-mode fiber eliminates most atmospheric effects except for *fringe jitter,* which is due to differential atmospheric piston. The fringe jitter can introduce a bias into the measured visibility which must be estimated and corrected. The first-difference variance phase $\sigma_{\Delta\phi}$ gives an estimate of the jitter which can be used to derive a small multiplicative correction (Colavita 1998). The jitter correction for these FU Orionis data ranges from 0.94 ± 0.05 to 0.98 ± 0.03.

The calibrator stars are used to estimate the system visibility. The Hipparcos catalogue (Perryman et al. 1997) provides the spectral type and parallax for each calibrator, from which we estimated their angular diameters. The calibrators are assumed to have uniform surface brightness. The results are not sensitive to this assumption since the calibrator stars are chosen to have diameters much smaller than the interferometer resolution. The system visibilities are fairly constant for each night (see Section 3.2) showing that the instrument is rather stable, with $V^2_{\rm inst} \sim 0.87 \pm 0.02$.

Figure 1 displays the calibrated square visibilities V^2 for FU Orionis and its calibrators. The error bars are estimated from the contributions of the fluctuations of $V^2_{\rm raw}$ between subsamples of the individual scans, the jitter correction errors, and the instrumental visibility errors.

3.2. Data Quality Measures

Because the magnitude of FU Ori is close to the limiting magnitude of the PTI, we present the following unusually detailed discussion of the data quality. We have run several checks on the data to validate the results and the associated uncertainties. The corresponding plots are displayed in Fig. 2 and discussed below:

Visibility vs Stellar Flux. One might imagine that for an object at the detection limit, flux-dependent terms might become important in the calibration of the visibilities. Figure 2a displays V^2 data for FU Orionis and its calibrators and shows no decrease in visibility as a function of flux.

Read-out Noise. The observations of FU Ori are dominated by the detector read-out noise. Colavita (1998) assesses the expected uncertainties for PTI data. In our observations, the flux $N \sim 20$ photoelectrons per 10ms read-out, the read noise $\sigma \sim 16$ e$^-$ and the total number of samples $M = 12500$ (5 spectral channels combined incoherently each with 25 s of 10-ms frames) lead to $\sigma_{V^2} = 0.113$ for each 25-s measurements. The observed statistical error of 0.05 for a 125-s long observation is consistent with the errors computed statistically for $V^2_{\rm raw}$.

Phase Jitter. The effect of the phase jitter due to imperfect tracking of the fringe as it moves due to atmospheric turbulence (piston) is to introduce a bias which decreases the estimated visibility. Colavita (1998) shows that the jitter is related to the convolution of the variance, $\sigma^2_{\Delta\phi}$, of the differences between successive phase measurements with the power spectrum of the piston disturbance. If the power spectrum is dominated by frequencies higher than 10 ms, one finds that the visibility bias is $e^{-C_\Gamma \sigma^2_{\Delta\phi}}$ with $C_\Gamma = 0.04$. A plot of the jitter-corrected V^2 versus $\sigma_{\Delta\phi}$ (Fig. 2b) shows no systematic dependence of the visibility on the size of the jitter. We conclude that the data are free of jitter bias. The errors introduced by this jitter correction are of the order of 0.05 for nights 305 and 306, 0.03 for night 307 and 0.04 for nights 309 to 311.

Flux Ratio. The flux-ratio correction accounts for the difference in fluxes between the two arms of the interferometer, which occurs mainly as a result of optical vignetting. This vignetting results in a bias that decreases the visibility estimation. If this effect is large, measured visibilities should decrease as the correction ratio increases. Figure 2c displays the flux-ratio correction versus V^2. Except for the points measured at 10:54 on night 305 and at 10:39 on night 306 that show strong departures, we see no flux-correction effect in the data and have made no correction for it.

Incoherent Data vs Coherent Data. We processed the coherent data in the same manner as the incoherent data. The effect of jitter is much more important in these data[2], giving rise to larger uncertainties. The two different measurements are consistent within the uncertainties (Fig. 2d), with the coherent visibilities being slightly smaller ($V^2 \sim 0.8$).

White-Light Data. The white light channel is not spatially filtered by a single-mode fiber. This leads to low visibilities, $V^2 \sim 0.3 - 0.4$, and biases that are difficult to understand. We did not use these measurements to estimate FU Orionis visibilities. However, the FU Orionis raw square visibilities in white light measurements are always smaller than the calibrator values with a ratio of the order of 0.6-0.7, consistent with the spectrometer data.

---

[2] $C_\Gamma \sim 0.4 \pm 0.2$, measured by fitting $K \exp(-C_\Gamma \sigma^2_{\Delta\phi})$ to the data.

4. Results and interpretation

The calibrated visibilities of FU Orionis display no clear trends with time, projected baseline, or projected angle. We have therefore adopted an averaged visibility value[3] of $V^2 = 0.72 \pm 0.07$ for an averaged projected baseline of 103 ± 5 m and projected angle of $64 \pm 9°$. Because of the very limited coverage of the visibility space, the current observations cannot provide images of the FU Orionis system which would reveal its morphological structure. The PTI at $\lambda = 2.2\mu$m has a spatial resolution of $\lambda/B = 4.4$ mas, corresponding to 2 AU at a distance of 450 pc. *The principal result of this paper is that FU Orionis is clearly resolved on this angular scale.*

As described in the introduction, the double-peaked absorption line profiles, wavelength-dependent spectral types, and excess infrared emission offer fairly strong evidence for the presence of an active accretion disk. Although there is strong circumstantial evidence for the disk scenario, there has not yet been a direct detection of a physical structure of the predicted extent and we therefore briefly discuss several alternative interpretations of the new observational result.

Resolved stellar surface. The angular diameter of a uniformly emitting stellar surface that would give the observed visibility is 1.55 mas, corresponding to a linear diameter of 0.7 AU or 150 $R_\odot$ at the distance of FU Orionis. With a 500 $L_\odot$ luminosity, such a star would exhibit an effective temperature of 2200 K. This interpretation is inconsistent with the observed spectral type by Kenyon, Hartmann, & Hewett (1988, hereafter KHH88), who find spectral types ranging from F7 I for the CN λ3860 lines to K3 for the TiO λ7050 bands. We therefore consider it unlikely that the PTI observations are resolving a bare stellar photosphere.

Resolved binary system. A second phenomenon that could explain the observed visibility is the presence of a stellar companion. Here we consider a model in which FU Orionis consists of a pair of unresolved stars with angular separation s and magnitude difference ΔK. Figure 3 shows the values for the binary parameters permitted by our visibility measurement. The maximum value of ΔK consistent with the observations is found to be 2.7 ± 0.5 mag, and the smallest separation s is 0.8 ± 0.1 mas, i.e. 0.35 ± 0.05 AU at the distance of FU Ori.

High resolution spectroscopy (Hartmann & Kenyon 1985, hereafter HK85) reveals double-peaked photospheric lines in FU Ori spectrum that, at least in principle, could

[3]Obtained without the two aberrated points mentioned in §3.2. With all points, the value is $V^2 = 0.71 \pm 0.08$.

originate from a binary system with an estimated separation $s \leq 0.25(M \sin^2 i/1\ \mathrm{M}_\odot)$ AU. Such a model is also compatible with our present data set if the total mass of the system is ≥ 1.4 M$\odot$, although a considerably more extensive set of observations covering a wide range of projected baseline angles could rule it out. We note that HK85 and KHH88 have favored the accretion disk model to explain the line doubling, because it also succeeds in modeling the SED and the change of spectral type and line profiles with the wavelength.

Dust halo model. Many YSOs show large amounts of scattered light in visible and near-IR images (e.g. Nakajima & Golimowski 1995; Burrows et al. 1996). DeWarf & Dyck (1993) fitted their 2.2 μm speckle observations of FU Orionis with a Gaussian halo some 0.07 arcsec (35 AU) in diameter, although their data were also consistent with an unresolved object. The PTI data can be fitted by an unresolved star surrounded by a scattering envelope of uniform brightness. The envelope would account for $\sim 15\%$ of the total 2.2 μm flux. Its size is poorly constrained by the PTI visibility measurement: the visibility is insensitive to the size if it is larger than ~ 10 mas. We argue below that depending on the size of the halo, the dust may be seen by direct radiation rather than scattered light.

The equilibrium temperature of dust close to FU Ori is roughly 270 K$(L/1\ \mathrm{L}_\odot)^{1/4}(r/1\ \mathrm{AU})^{-1/2 \text{ to } -3/4}$, depending on the geometrical arrangement of the dust and heating source (Friedjung 1985). The temperature of dust 2 AU from this $L \sim 500\ \mathrm{L}_\odot$ object, i.e. at the minimum physical distance resolved by these observations, is ~ 750 K; at the 17 AU radius of the halo suggested by the speckle results it is ~ 310 K. Hot material close to the star would emit strongly at 2.2μm and with an optical depth roughly 5 times greater than the scattering optical depth (Draine & Lee 1984). The ratio of emitted light to scattered light is roughly:

$$\frac{B_\nu(T_{\rm gr}(r))}{\omega B_\nu(T_{\rm eff})(r/R)^{-2}}$$

where ω is the albedo (~ 0.2, Draine & Lee 1984), r is the distance to center, R and $T_{\rm eff}$ are the equivalent radius and effective temperature of the central source. With $R = 4\ \mathrm{R}_\odot$ and $T_{\rm eff} = 6000 - 8000$K, the ratio is much larger than 1 at 2 AU and much smaller than 1 at 17 AU. While a detailed radiative transfer model must be used to assess the relative importance of scattering and thermal emission, we regard thermal emission as likely to be dominant if the radius of the putative dust halo is much smaller than ~ 10 AU, whereas scattering will be important if the radius is much larger.

Accretion disk model. Following MB95, thermal emission from an accretion disk of the type proposed by KH85 and KHH88 is expected to be resolved in the PTI data, with approximately the observed fringe visibility. We computed a disk model with a surface temperature distribution proportional to $r^{-3/4}$ to fit the observed SED.[4] The model implies an accretion rate of $\dot{M} \sim 6 \times 10^{-5}$ $M_\odot$ yr^{-1} for a 1 $M_\odot$ star, an $A_V \sim 1$ mag and an inclination angle of $i \sim 30°$. The resulting synthetic image at 2.2μm is displayed in Figure 4 (middle panel) together with the predicted visibility curves for the major and minor axis (right panel). Our interferometric data are in very good agreement with the accretion disk model. However, the precision of the individual visibility measurements is inadequate to constrain the position angle for the disk.

5. Conclusions

We have resolved a young stellar object for the first time using long-baseline interferometry in the near-infrared, achieving a projected spatial resolution of 2 AU using the *Palomar Testbed Interferometer*. Although the single visibility measurement presented here can only offer limited constraints on existing astrophysical models, it is reassuringly consistent with the accretion disk which was inferred from earlier spectral and spectrophotometric data. More sensitive multi-aperture infrared interferometers like the *Keck Interferometer* and the *Very Large Telescope Interferometer* (VLTI), now under construction, will soon enable more robust studies by producing true images of FUor disks with $\sim$ 2 AU resolution, and even more detailed images of the disks of less luminous T Tauri stars.

REFERENCES

Allen D.A. 1973, MNRAS 161, 145

Burrows C.J., et al. 1996, ApJ 473, 437

Colavita M.M., et al. 1994, Proc. SPIE 2200, 89

Colavita M.M. 1998, submitted

DeWarf L.E., & Dyck H.M. 1993, AJ 105, 2211

Draine B.T., & Lee H.M. 1984, ApJ 285, 89

Friedjung M. 1985, A&A 146, 366

[4]Photometry data from Allen (1973), Glass & Penston (1974), KHH88 and IRAS.

Glass I.S., & Penston M.V. 1974, MNRAS 167, 237

Hartmann L., & Kenyon S.J. 1996, ARA&A 34, 207

Hartmann L., & Kenyon S.J. 1985, ApJ 299, 462 (HK85)

Herbig G.H. 1966, Vistas Astron 8, 109

Kenyon S.J., & Hartmann L. 1991, ApJ 383, 664

Kenyon S.J., Hartmann L., & Hewett R. 1988, ApJ 325, 231 (KHH88)

Malbet F., & Bertout C. 1995, A&AS 113, 369 (MB95)

Nakajima T., & Golimowski D.A. 1995, AJ 109, 1181

Perryman M.A.C., et al. 1997, A&A 323, L49

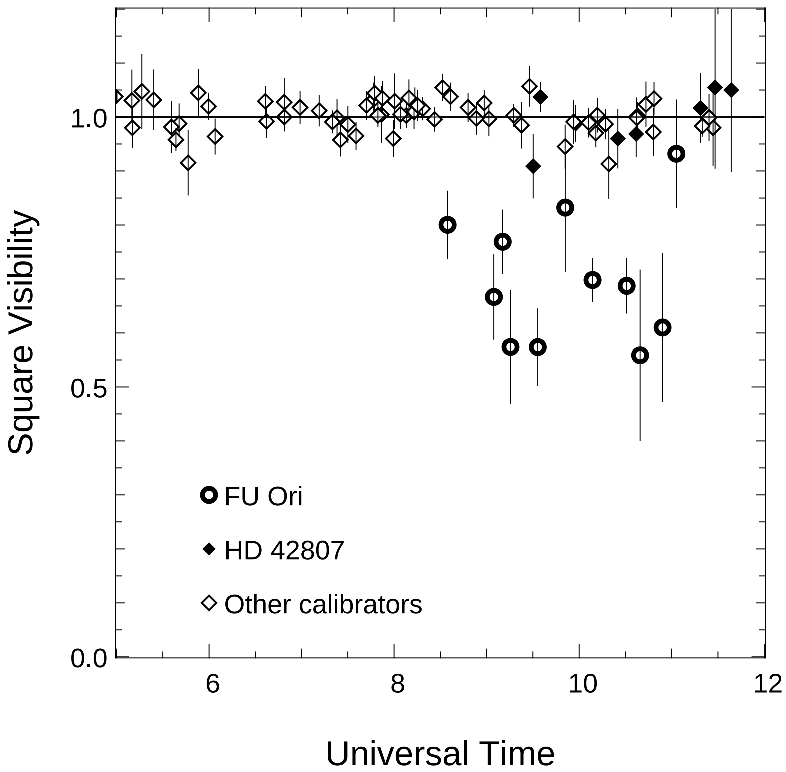

Fig. 1.— Calibrated square visibilities of FU Ori (open circles) and its calibrators (diamonds) from several nights. The local calibrator HD 42807 is displayed in filled diamonds.

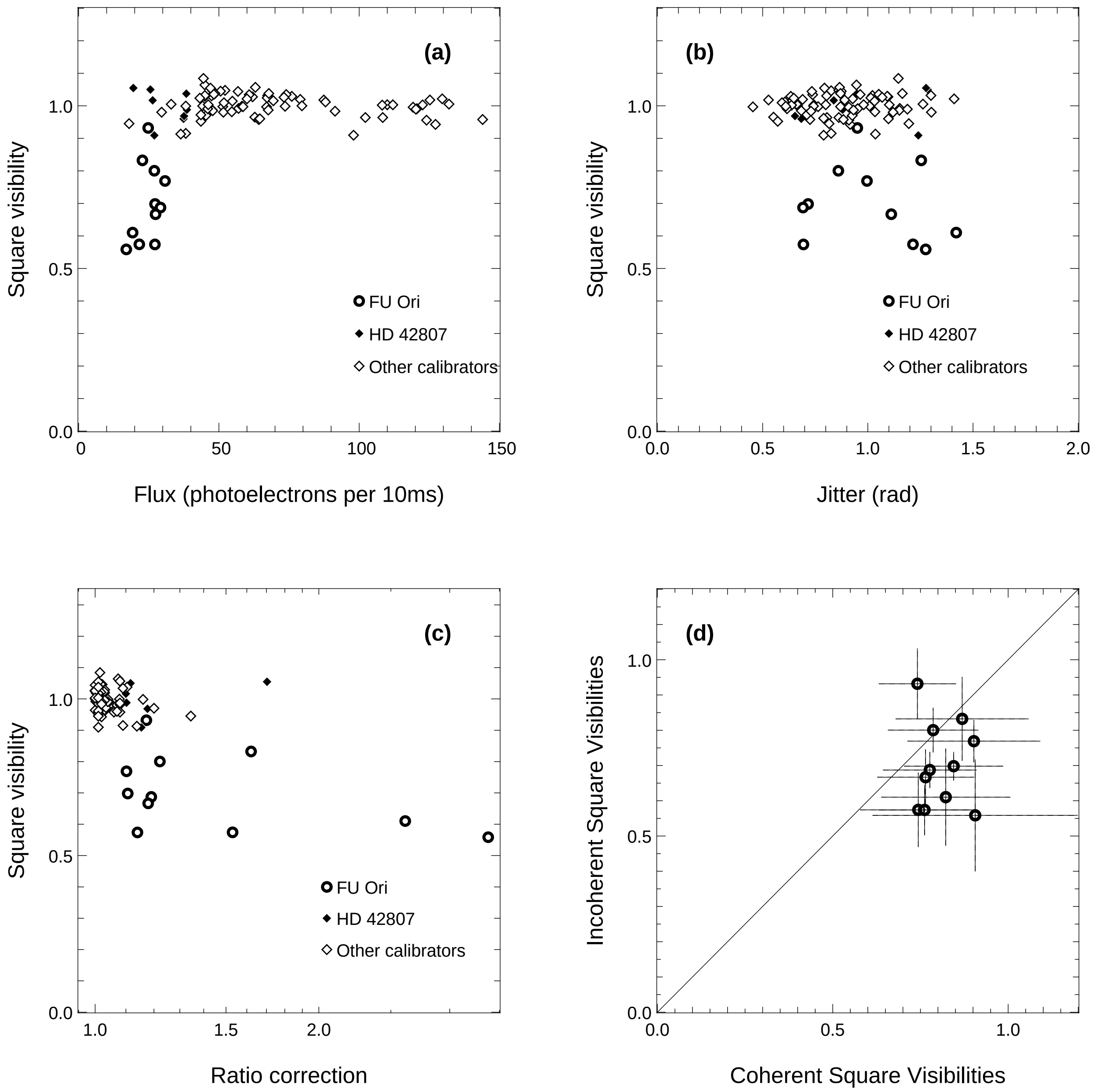

Fig. 2.— Data quality measures. Square visibilities versus flux in units of photoelectrons per 10 ms readout (Panel a), versus jitter (Panel b), versus ratio correction (Panel c). Incoherent (y-axis) versus coherent (x-axis) square visibilities (Panel d); the crosses represent the error bars.

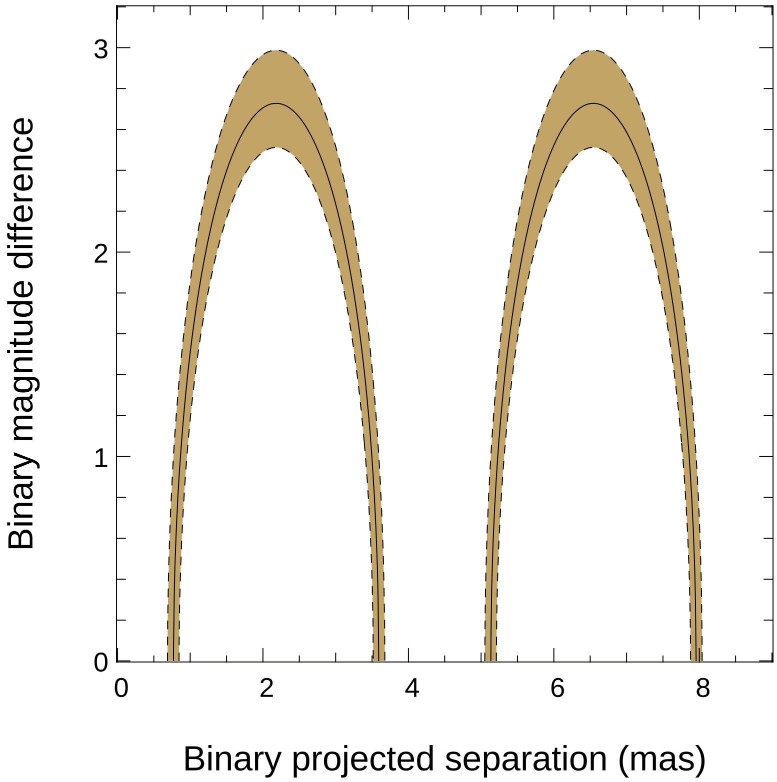

Fig. 3.— Binary scenario. The K magnitude difference versus the separation projected on the baseline. The colored region is permitted.

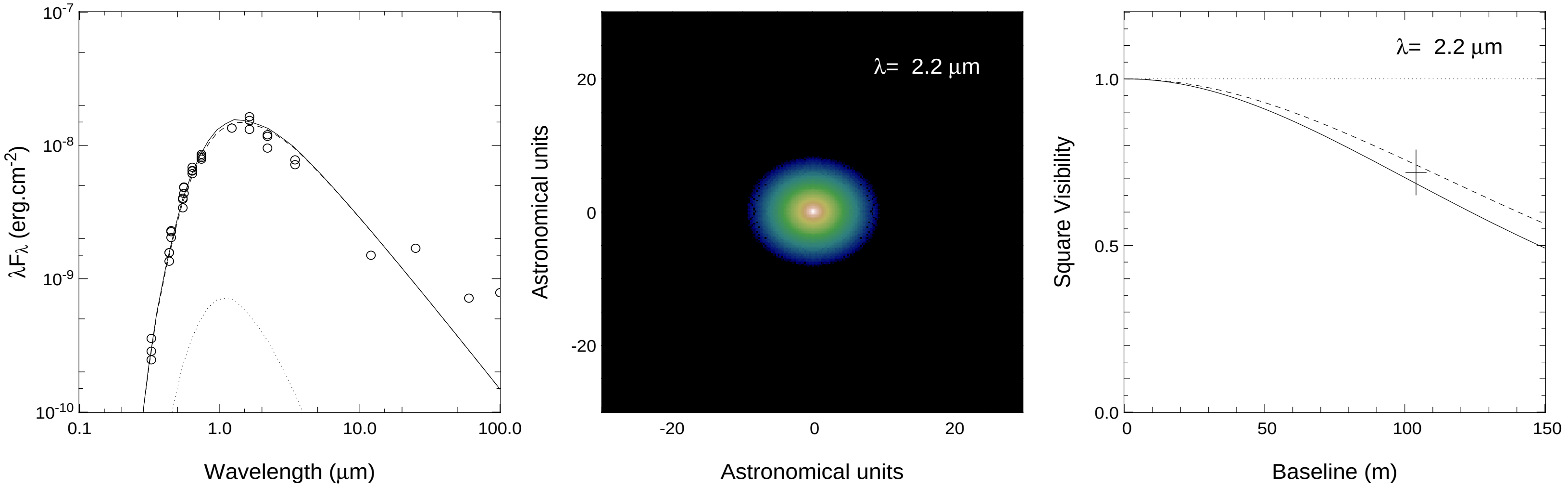

Fig. 4.— Accretion disk model. Left panel displays the spectral energy distribution from litterature data (circles), of the accretion disk model (dashed line), the star (dotted line) and the whole system (solid line), middle panel the synthetic image of the accretion disk at 2.2μm, and right panel the visibility curves of the accretion disk model for the x and y directions (respectively solid and dashed lines). The result of our PTI observation of FU Ori is placed on the figure with its error bars.